Chapter 5

Reconfigurable Intelligent Surfaces Assisted Hybrid NOMA System*

*Part of this work has been published as:

M. Hemanta Kumar, Sanjeev Sharma, M. Thottappan, and Kuntal Deka. "Reconfigurable Intelligent Surfaces Assisted hybrid NOMA System", *IEEE Communications Letters* 27, no. 1 (2023): 357-361

5.1 Introduction

In this chapter, more users are considered to be distributed at the cell edge than the cell center in device-to-device communication. In such a scenario, some users are paired using conventional NOMA, and the remaining cell-edge users are served by OMA and remain unpaired, and these serve by OMA. This system is called as hybrid-NOMA (HNOMA). Consequently, it degrades the spectral efficiency of a network. Further, the user pairing of users consider the difference between the channel gains or power allocations of any two users is significant, which may reduce the capacity of the system due to interference. The multiuser system has a higher computational complexity and degrades the decoding performance as it employs multiple times SIC due to more number of users increases. Therefore, a RIS-assisted user-pairing hybrid NOMA system (PR-HNOMA) is proposed to alleviate the aforementioned issues.

The main contributions of the chapter is summarized below:

- In the PR-NOMA, users are distributed into multiple clusters, and each cluster has three users, where BS serves one near user (NU) $\mathcal{U}_1$ and two far users (FUs) $\mathcal{U}_2$ and $\mathcal{U}_3$ through direct link and RIS.
- A joint optimization of transmit antennas beamforming and reflecting elements phase at the BS and RIS, respectively, implemented by using SDR and AO techniques.
- Therefore, the optimization leads to the sum-rate performance maximization of RIS assisted hybrid NOMA system for the practical imperfect SIC (ISIC) scenario.

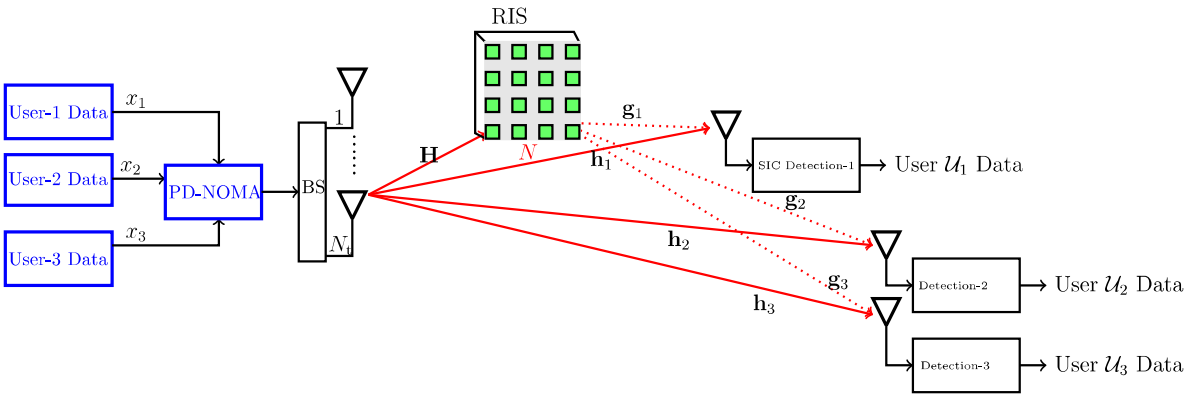

FIGURE 5.1: The proposed RIS-assisted hybrid NOMA system model.

- Next, the proposed PR-HNOMA system with conventional RIS assisted HNOMA (R-HNOMA), RIS assisted NOMA (R-CNOMA), and RIS assisted OMA (R-OMA) systems, are compared.
- Finally, the sum rate of RIS-assisted systems with different transmit beamforming schemes like BS-User and BS-RIS channel-based maximum ratio transmission (MRT).

This chapter is organized as follows. In Section 5.2, the proposed RIS-assisted hybrid NOMA system is presented. The joint active and passive beamforming techniques are presented in Section 5.3. Simulation results are presented in Section 5.4, and the Summary of the proposed work is discussed in Sections 5.5.

5.2 Proposed System Model

This section describes the system model for PR-NOMA in detail and compares it with benchmark R-HNOMA and R-CNOMA models.

5.2.1 Proposed RIS-assisted HNOMA (PR-HNOMA)

A single cluster having three users is considered, as shown in Figure 5.1. The proposed downlink RIS-assisted HNOMA (PR-HNOMA) system is equipped with N_{t} transmit antennas, and each user has a single antenna. The RIS panel consists of N reflecting elements, as depicted in Figure 5.1. Let the total available bandwidth be B Hz. In the PR-HNOMA system, bandwidth $B_1 = \delta B$ is assigned for pairing the NU $\mathcal{U}_1$ and FU $\mathcal{U}_2$, and the remaining bandwidth $B_2 = B - \delta B$ is allocated for pairing NU $\mathcal{U}_1$ and FU $\mathcal{U}_3$, where $0 < \delta < 1$. The value of δ is assigned according to the channel gain of $\mathcal{U}_2$ and $\mathcal{U}_3$. Moreover, each user receives signals from both direct and reflected links from the BS and RIS, respectively, as shown in Figure 5.1.

The channel between the BS and RIS follows the Rician flat fading which is given as,

$$\mathbf{H} = \frac{1}{\sqrt{d_{\mathrm{BR}}^{\beta}}} \left(\sqrt{\frac{\mathrm{K}}{\mathrm{K}+1}} \tilde{\mathbf{H}} + \sqrt{\frac{1}{\mathrm{K}_1+1}} \bar{\mathbf{H}} \right) \in \mathbb{C}^{N \times N_{\mathrm{t}}}, \tag{5.1}$$

where, d_{BR} is the distance between the BS and RIS, and β represents the path loss exponent. $\tilde{\mathbf{H}}$ and $\bar{\mathbf{H}}$ denote the line-of-sight (LoS) and non-LoS (NLoS) components, respectively with Rayleigh flat fading, and K is the Rician factor. Similarly, the channel vectors between RIS and users $\mathcal{U}_i$, $i \in 1, 2, 3$ are given as,

$$\mathbf{g}_i = \frac{1}{\sqrt{d_{\mathrm{RU_i}}^{\beta}}} \sqrt{\frac{\mathrm{K}_i}{\mathrm{K}_i+1}} \tilde{\mathbf{g}}_i + \sqrt{\frac{1}{\mathrm{K}_i+1}} \bar{\mathbf{g}}_i \in \mathbb{C}^{N \times 1}, \tag{5.2}$$

where, $\tilde{\mathbf{g}}_i$ and $\bar{\mathbf{g}}_i$ are the LoS and NLoS components with Rayleigh flat fading, and K_i denotes the Rician factor. $d_{\mathrm{R}\mathcal{U}_i}$ denotes the distance between the RIS and user $\mathcal{U}_i$.

Further, the channel for the direct link between the BS to user $\mathcal{U}_i$ is denoted by $\mathbf{h}_i \in \mathbb{C}^{N_{\mathrm{t}} \times 1}$. These channels follow Rayleigh-flat fading which are independent and

identically distributed (iid) with $\mathbf{h}_i \sim \mathcal{CN}(0, \sigma_{\mathrm{i}}^2)$. The NU and FU's distances from the BS are $d_{\mathrm{B}\mathcal{U}_1}$, $d_{\mathrm{B}\mathcal{U}_2}$ and $d_{\mathrm{B}\mathcal{U}_3}$, respectively. Let η be the path loss component of the direct link, and the channel gain of $\mathcal{U}_1$ is higher than $\mathcal{U}_2$ and $\mathcal{U}_3$, i.e., $||\mathbf{h}_1||^2 > ||\mathbf{h}_2||^2 \simeq ||\mathbf{h}_3||^2$. Further, $\mathcal{U}_2$ and $\mathcal{U}_3$ are close to each other and are not paired.

In PR-HNOMA system, initially pairing of $\mathcal{U}_1$ and $\mathcal{U}_2$ is done over the BW B_1, as shown in Figure 5.2[a]. The received signal at user $\mathcal{U}_1$ and $\mathcal{U}_2$ is expressed as,

$$y_1 = \mathbf{f}_1 \left(\mathbf{w}_1 \sqrt{\alpha_1 \mathrm{P_t}} x_1 + \mathbf{w}_2 \sqrt{\alpha_2 \mathrm{P_t}} x_2 \right) + n_1, \tag{5.3}$$

$$y_2 = \mathbf{f}_2 \left(\mathbf{w}_1 \sqrt{\alpha_1 \mathrm{P_t}} x_1 + \mathbf{w}_2 \sqrt{\alpha_2 \mathrm{P_t}} x_2 \right) + n_2, \tag{5.4}$$

where, x_1 and x_2 are the binary-phase shift keying (BPSK) symbols. α_1 and α_2 are power coefficients assigned to $\mathcal{U}_1$ and $\mathcal{U}_2$, respectively, according to their channel gains. P_t is the total transmit power available at the BS. Further, $\mathbf{f}_1 = \left({\mathbf{g}_1}^H \mathbf{\Phi} \mathbf{H} + {\mathbf{h}_1}^H \right)$ and $\mathbf{f}_2 = \left({\mathbf{g}_2}^H \mathbf{\Phi} \mathbf{H} + {\mathbf{h}_2}^H \right)$ denote the effective channels between the BS and users $\mathcal{U}_1$, $\mathcal{U}_2$, respectively. $\mathbf{w}_1 \in \mathbb{C}^{N_t \times 1}$ and $\mathbf{w}_2 \in \mathbb{C}^{N_t \times 1}$ are beamforming vectors. $\mathbf{\Phi} \in \mathbb{C}^{N \times N}$ is a diagonal matrix as $\mathbf{\Phi} = \mathrm{diag}[A_1 \mathrm{e}^{\phi_1}, A_2 \mathrm{e}^{\phi_2}, \ldots, A_N \mathrm{e}^{\phi_N}]$. $A_n \in (0, 1]$ denotes the reflection coefficients, and in general $|A_n| = 1$ and $\phi_n \in (0, 2\pi]$ $\forall n$. $n_i, i = 1, 2$ is the white Gaussian noise with $n_i \sim \mathcal{CN}(0, N_0)$.

The received SINR of $\mathcal{U}_1$ after applying SIC is given as,

$$\gamma_{\mathcal{U}_1} = \frac{\left| \mathbf{f}_1 \mathbf{w}_1 \right|^2 \alpha_1 \mathrm{P_t}}{\left| \tilde{\mathbf{f}}_1 \mathbf{w}_2 \right|^2 \alpha_2 \mathrm{P_t} + N_0}. \tag{5.5}$$

where, $\tilde{\mathbf{f}}_1 \sim \mathcal{CN}(0, \zeta_1)$ [96]. ζ_1 is SIC parameter, and $\zeta_1 = 0$ and $\zeta_1 = 1$ denote the perfect SIC and no SIC, respectively. The SINR $\gamma_{\mathcal{U}_2}$ of $\mathcal{U}_2$ is expressed as,

$$\gamma_{\mathcal{U}_2} = \frac{\left| \mathbf{f}_2 \mathbf{w}_2 \right|^2 \alpha_2 \mathrm{P_t}}{\left| \mathbf{f}_2 \mathbf{w}_1 \right|^2 \alpha_1 \mathrm{P_t} + N_0}. \tag{5.6}$$

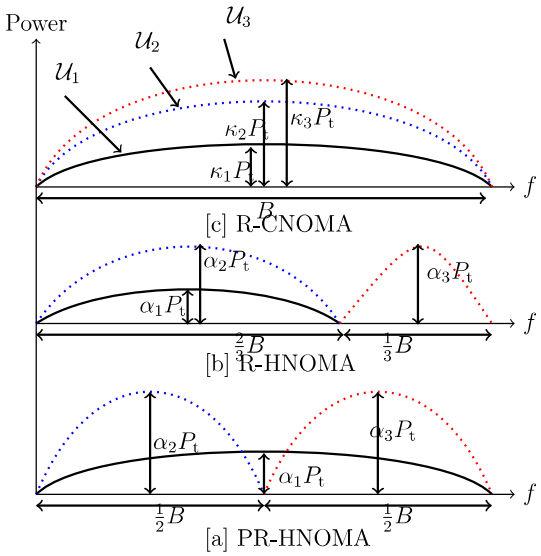

FIGURE 5.2: Three different NOMA scenarios.

The sum-rate of paired $\mathcal{U}_1$ and $\mathcal{U}_2$ over BW B_1 is expressed as,

$$\mathcal{R}_{B_1} = B_1 \log_2 (1 + \gamma_{\mathcal{U}_1}) + B_1 \log_2 (1 + \gamma_{\mathcal{U}_2}) . \tag{5.7}$$

Next, the sum-rate of paired $\mathcal{U}_1$ and $\mathcal{U}_3$ over bandwidth B_2 is

$$\mathcal{R}_{B_2} = B_2 \log_2 (1 + \gamma_{\mathcal{U}_1}) + B_2 \log_2 (1 + \gamma_{\mathcal{U}_3}) , \tag{5.8}$$

where $\gamma_{\mathcal{U}_3}$ is the SINR of $\mathcal{U}_3$ as $\gamma_{\mathcal{U}_3} = \frac{|\mathbf{f}_3 \mathbf{w}_3|^2 \alpha_3 \mathrm{P_t}}{|\mathbf{f}_3 \mathbf{w}_1|^2 \alpha_1 \mathrm{P_t} + N_0}$ with $\mathbf{f}_3 = \left(\mathbf{g}_3{}^H \mathbf{\Phi} \mathbf{H} + \mathbf{h}_3{}^H\right)$, and the total sum-rate of PR-HNOMA is $\mathcal{R}_{B_1} + \mathcal{R}_{B_2}$.

5.2.2 RIS assisted HNOMA (R-HNOMA)

In R-NOMA, $\mathcal{U}_1$ and $\mathcal{U}_2$ communicate using NOMA, and $\mathcal{U}_3$ uses OMA with the bandwidth of $\frac{2}{3}B$ and $\frac{1}{3}B$, respectively, as shown in Figure5.2 [b]. The sum-rate of

R-HNOMA is given as

$$\mathcal{R}_{\text{HNOMA}} = \frac{2}{3}B\left[\log_2\left(1+\text{SNR}_1\right)+\log_2\left(1+\text{SINR}_2\right)\right] + \frac{1}{3}B\log_2\left(1+\text{SNR}_3\right), \tag{5.9}$$

where, SNR_1 is SNR of NOMA $\mathcal{U}_1$ is,

$$\gamma_{\mathcal{U}_1}^{N} = \frac{3\left|\mathbf{f}_1\mathbf{w}_1\right|^2\text{P}_\text{t}}{(2/3)BN_0}, \text{ and} \tag{5.10}$$

SINR_2 is SINR of NOMA $\mathcal{U}_2$ is

$$\gamma_{\mathcal{U}_2}^{N} = \frac{3\left|\mathbf{f}_2\mathbf{w}_2\right|^2\alpha_2\text{P}_\text{t}}{\left|\mathbf{f}_2\mathbf{w}_1\right|^2\alpha_1\text{P}_\text{t}+(2/3)BN_0}. \tag{5.11}$$

The SNR_3 is SNR of OMA user is

$$\gamma_{\mathcal{U}_3}^{O} = \frac{\left|\mathbf{f}_3\mathbf{w}_3\right|^2\text{P}_\text{t}}{(1/3)BN_0}, \tag{5.12}$$

5.2.3 RIS-assisted Conventional NOMA (R-CNOMA)

In R-CNOMA, $\mathcal{U}_1, \mathcal{U}_2$ and $\mathcal{U}_3$ communicate using NOMA technique with bandwidth B. The sum-rate of R-CNOMA given as

$$\mathcal{R}_{\text{CNOMA}} = B\log_2\left(1+\gamma_{\mathcal{U}_1}^{\text{C}}\right)+B\log_2\left(1+\gamma_{\mathcal{U}_2}^{\text{C}}\right)+B\log_2\left(1+\gamma_{\mathcal{U}_3}^{\text{C}}\right), \tag{5.13}$$

where, $\gamma_{\mathcal{U}_1}^{\text{C}}$ is SNR of $\mathcal{U}_1$ is expressed as,

$$\gamma_{\mathcal{U}_1} = \frac{\left|\mathbf{f}_1\mathbf{w}_1\right|^2\kappa_1\text{P}_\text{t}}{N_0}. \tag{5.14}$$

The $\gamma_{\mathcal{U}_2}^{\mathrm{C}}$ and $\gamma_{\mathcal{U}_3}^{\mathrm{C}}$ are the SINR of $\mathcal{U}_2$ and $\mathcal{U}_3$, respectively, and it represents as,

$$\gamma_{\mathcal{U}_2} = \frac{\left|\mathbf{f}_2\mathbf{w}_2\right|^2 \kappa_2 \mathrm{P_t}}{\left|\mathbf{f}_2\mathbf{w}_1\right|^2 \kappa_1 \mathrm{P_t} + \left|\mathbf{f}_2\mathbf{w}_3\right|^2 \kappa_3 \mathrm{P_t} + N_0}, \text{and} \tag{5.15}$$

$$\gamma_{\mathcal{U}_2} = \frac{\left|\mathbf{f}_3\mathbf{w}_3\right|^2 \kappa_3 \mathrm{P_t}}{\left|\mathbf{f}_3\mathbf{w}_1\right|^2 \kappa_1 \mathrm{P_t} + \left|\mathbf{f}_3\mathbf{w}_3\right|^2 \kappa_3 \mathrm{P_t} + N_0}. \tag{5.16}$$

5.3 Joint Active and Passive Beamforming Optimization

In this section, we maximize the sum-rate of the proposed PR-HNOMA by jointly optimizing the transmit beamforming at the BS and phase shift at RIS. The received SNR of $\mathcal{U}_1$ in paired $\mathcal{U}_1$- $\mathcal{U}_2$ after considering the perfect SIC is given as

$$\gamma_{\mathcal{U}_1} = \left|\left(\mathbf{g}_1{}^H \mathbf{\Phi}\mathbf{H} + \mathbf{h}_1{}^H\right)\mathbf{w}_1\right|^2 \gamma_1, \tag{5.17}$$

where $\gamma_1 = \frac{\alpha_1 \mathrm{P_t}}{N_0}$ is transmit SNR. The SNR $\gamma_{\mathcal{U}_1}$ is maximized by applying joint beamforming and phase optimization as

$$(\mathrm{P1}): \ \min_{\mathbf{w}_1, \boldsymbol{\phi}} \ \|\mathbf{w}_1\|^2 \tag{5.18}$$

$$\text{s.t.} \ \left|\left(\mathbf{g}_1{}^H \mathbf{\Phi}\mathbf{H} + \mathbf{h}_1{}^H\right)\mathbf{w}_1\right|^2 \geq \frac{\gamma_{\mathcal{U}_1}}{\gamma_1}, \tag{5.19}$$

$$0 \leq \phi_n \leq 2\pi, \quad n = 1, \cdots, N. \tag{5.20}$$

The above problem (P1) is non-convex since $\left|\left(\mathbf{g}_1{}^H \mathbf{\Phi}\mathbf{H} + \mathbf{h}_1{}^H\right)\mathbf{w}_1\right|^2$ is not jointly concave with respect to $\mathbf{w}_1$ and $\boldsymbol{\phi}$. Therefore, (P1) can be optimized using SDR and AO techniques [93].

5.3.1 SDR-Based Solution

Initially, SDR is applied to solve (P1). However, the maximum ratio transmission (MRT) [97] beamforming is used for given phase shift as $\mathbf{w}_1^* = \sqrt{\mathrm{P_t}}\frac{\left(\mathbf{g_1}^H\mathbf{\Phi}\mathbf{H}+\mathbf{h_1}^H\right)^H}{\left\|\left(\mathbf{g_1}^H\mathbf{\Phi}\mathbf{H}+\mathbf{h_1}^H\right)\right\|}$. By substituting $\mathbf{w}_1^*$, the (P1) is converted as

$$(\mathrm{P2}): \min_{\mathrm{P_t},\boldsymbol{\phi}} \ \|\mathrm{P_t}\| \tag{5.21}$$

$$\text{s.t. } \left\|\left(\mathbf{g_1}^H\mathbf{\Phi}\mathbf{H}+\mathbf{h_1}^H\right)\right\|^2 \geq \frac{\gamma_{\mathcal{U}_1}}{\gamma_1}, \tag{5.22}$$

$$0 \leq \phi_n \leq 2\pi, \quad n = 1, \cdots, N. \tag{5.23}$$

Therefore, the optimal transmit power in (5.21) is $\mathrm{P_t^*} = \frac{\gamma_{\mathcal{U}_1}}{\gamma_1\left\|\left(\mathbf{g_1}^H\mathbf{\Phi}\mathbf{H}+\mathbf{h_1}^H\right)\right\|^2}$. Furthermore, $\mathrm{P_t}$ is minimized by maximizing the effective channel gain as

$$(\mathrm{P2.1}): \max_{\boldsymbol{\phi}} \ \left\|\left(\mathbf{g_1}^H\mathbf{\Phi}\mathbf{H}+\mathbf{h_1}^H\right)\right\|^2 \tag{5.24}$$

$$\text{s.t. } 0 \leq \phi_n \leq 2\pi, \forall n. \tag{5.25}$$

The above problem (5.24) is still non-convex. Therefore, it is converted into quadratically constrained quadratic program (QCQP) [98] by changing the variables. Let $\mathbf{\Psi} = \mathrm{diag}(\mathbf{g_1}^H)\mathbf{H}$ and $\mathbf{r}^H = [\mathbf{r}_1, \ldots, \mathbf{r}_N]^H$, where $\mathbf{r}_n = e^{j\phi_n}$. Thus, the problem (5.24) can be rewritten as,

$$(\mathrm{P2.2}): \max_{\boldsymbol{r}} \ \|\mathbf{r}^H\mathbf{\Psi} + \boldsymbol{h}_1^H\|^2 \tag{5.26}$$

$$\text{s.t. } |r_n|^2 = 1, \quad \forall n. \tag{5.27}$$

Further, the problem (5.26) can be reformulated homogeneous QCQP as

$$(\text{P2.3}) : \max_{\bar{\boldsymbol{r}}} \ \bar{\boldsymbol{r}}^H \boldsymbol{V} \bar{\boldsymbol{r}} + \|\boldsymbol{h}_1^H\|^2 \tag{5.28}$$

$$\text{s.t. } |\bar{r}_n|^2 = 1, \quad n = 1, \cdots, N+1, \tag{5.29}$$

where

$$\boldsymbol{V} = \begin{bmatrix} \boldsymbol{\Psi}\boldsymbol{\Psi}^H & \boldsymbol{\Psi}\boldsymbol{h}_1 \\ \boldsymbol{h}_1^H \boldsymbol{\Psi}^H & 0 \end{bmatrix}, \quad \bar{\boldsymbol{r}} = \begin{bmatrix} \boldsymbol{r} \\ 1 \end{bmatrix}. \tag{5.30}$$

Although, problem (5.28) is non-convex, it can be reduced to convex semidefinite program (SDP). Further, the problem (5.28) converted into $\text{tr}(\boldsymbol{V}\bar{\boldsymbol{r}}\bar{\boldsymbol{r}}^H)$, where $\boldsymbol{R} = \bar{\boldsymbol{r}}\bar{\boldsymbol{r}}^H$, which need to satisfy $\boldsymbol{R} \succeq 0$ and rank $(\boldsymbol{R}) = 1$. Thus, problem (5.28) is reduced to a convex problem as

$$(\text{P2.4}) : \max_{\boldsymbol{R}} \ \text{tr}(\boldsymbol{V}\boldsymbol{R}) + \|\boldsymbol{h}_1^H\|^2 \tag{5.31}$$

$$\text{s.t. } \boldsymbol{R}_{n,n} = 1, \quad n = 1, \cdots, N+1, \tag{5.32}$$

$$\boldsymbol{R} \succeq 0. \tag{5.33}$$

Therefore, problem (5.31) is convex SDP and it optimally solves using convex optimization solver CVX [99].

5.3.2 AO-Based Solution

AO technique of lower complexity than the SDR based optimization is used. Since, both transmit beamforming direction and transmit power are optimized in alternating manner to generate a desired solution without using CVX. The maximized SNR

under fixed beamforming $\mathbf{w}_1$ can be formulated as

$$(\text{P3}) : \max_{\mathbf{\Phi}} \left| \left(\mathbf{g}^H \mathbf{\Phi} \mathbf{H}_1 + \mathbf{h_1}^H \right) \mathbf{w}_1 \right|^2 \tag{5.34}$$

$$\text{s.t. } 0 \leq \phi_n \leq 2\pi, \forall n. \tag{5.35}$$

The above problem (P3) is non-convex. Moreover, it holds the following inequality

$$\begin{aligned} |(\mathbf{g}_1{}^H \mathbf{\Phi} \mathbf{H}_1 + \mathbf{h}_1{}^H)\mathbf{w}_1| &= |\mathbf{g}_1{}^H \mathbf{\Phi} \mathbf{H}_1 \mathbf{w}_1 + \mathbf{h}_1{}^H \mathbf{w}_1| \\ &\overset{(u)}{\leq} |\mathbf{g}_1{}^H \mathbf{\Phi} \mathbf{H}_1 \mathbf{w}_1| + |\mathbf{h}_1{}^H \mathbf{w}_1|. \end{aligned} \tag{5.36}$$

Thus, equality in (u) holds if and only if $\arg(\mathbf{g}_1{}^H \mathbf{\Phi} \mathbf{H}_1 \mathbf{w}_1) = \arg(\mathbf{h}_1{}^H \mathbf{w}_1) \triangleq \theta_0$. By considering $\mathbf{g}_1{}^H \mathbf{\Phi} \mathbf{H}_1 \mathbf{w}_1 = \mathbf{l}^H \mathbf{q}$ with $\mathbf{q} = \text{diag}(\mathbf{g}_1{}^H)\mathbf{H}_1 \mathbf{w}_1$ and $\mathbf{l} = [\text{e}^{\phi_1}, \ldots, \text{e}^{\phi_n}, \ldots, \text{e}^{\phi_N}]^H$, the problem (P3) can be reformulated as

$$(\text{P3}') : \quad \max_{\mathbf{l}} \quad |\mathbf{l}^H \mathbf{q}| \tag{5.37}$$

$$\text{s.t.} \quad |l_n| = 1, \ n = 1, \ \cdots, \ N, \tag{5.38}$$

$$\arg(\mathbf{l}^H \mathbf{q}) = \theta_0. \tag{5.39}$$

Therefore, the optimal solution of (P3′) without using CVX is given as $\mathbf{l}^* = \text{e}^{j(\theta_0 - \arg(\mathbf{q}))} = \text{e}^{j(\theta_0 - \arg(\text{diag}(\mathbf{g}_1{}^H)\mathbf{H}_1 \mathbf{w}_1))}$.

Further, the received SINR of user pairing $\mathcal{U}_1$- $\mathcal{U}_2$ under the imperfect SIC is maximized using the AO technique as

$$(\text{P4}) : \ \min_{\boldsymbol{w}} \ \sum_{k=1}^{K} \|\boldsymbol{w}_k\|^2 \tag{5.40}$$

$$\text{s.t.} \ \frac{|\boldsymbol{f}_k \boldsymbol{w}_k|^2}{\sum_{j \neq k}^{K} |\boldsymbol{f}_k \boldsymbol{w}_j|^2 + N_0} \geq \gamma_{\mathcal{U}_k}. \tag{5.41}$$

Let, $\mathrm{b}_{k,j} = \mathbf{h}_k{}^H \mathbf{w}_j$ and $\mathbf{g}_k{}^H \mathbf{\Phi} \mathbf{H} \mathbf{w}_j = \mathbf{q}^H \mathbf{a}_{k,j}$ with $\mathbf{q} = [\mathrm{e}^{\phi_1}, \ldots, \mathrm{e}^{\phi_N}]^H$ and $q_n = \mathrm{e}^{\phi_n}$. Therefore, problem (P4) is transformed to

$$\begin{aligned} &\text{Find } \boldsymbol{q} \\ &\text{s.t. } \frac{|\boldsymbol{q}^H \boldsymbol{a}_{k,k} + b_{k,k}|^2}{\sum_{j \neq k}^{K} |\boldsymbol{q}^H \boldsymbol{a}_{k,j} + b_{k,j}|^2 + N_0} \geq \gamma_{\mathcal{U}_k}, \\ &\quad |q_n| = 1, \quad n = 1, \cdots, N. \end{aligned} \tag{5.42}$$

The above constraints are non-convex, and the optimization problem can be converted into quadratic constraints. Thus, the optimal solution of phase matrix $\mathbf{\Phi}$ can be derived by eigenvalue decomposition procedure for rank one, and Gaussian randomization technique to get an approximate solution for non-rank one case [100]-[101].

5.3.3 Convergence of AO algorithm

In the AO technique, the problems (P3) and (P4) are solved alternatively in an iterative manner. Further, the algorithm starts by solving the problem (P3) for given ϕ and similarly we solve problem (P4) for given $\boldsymbol{w}$. Moreover, problem (P3) is always feasible for any arbitrary value of ϕ, due to the provided the rank one channel, but in the case of problem (P4) may not be true for arbitrary value of $\boldsymbol{w}$. The feasible solution of (P4) attains the value of (P2). Value of (P3) monotonically decreases and it saturates after few iterations, as observed in Figure 5.3. Moreover, the feasible solution of (P4) is obtained for the targeted SINR γ_k for the kth user. The transmitted power (P4) increases as target SINR increases [93]. The same is observed in Figure 5.4. Therefore, the proposed algorithm is converged, as observed in Figure 5.3 and Figure 5.4.

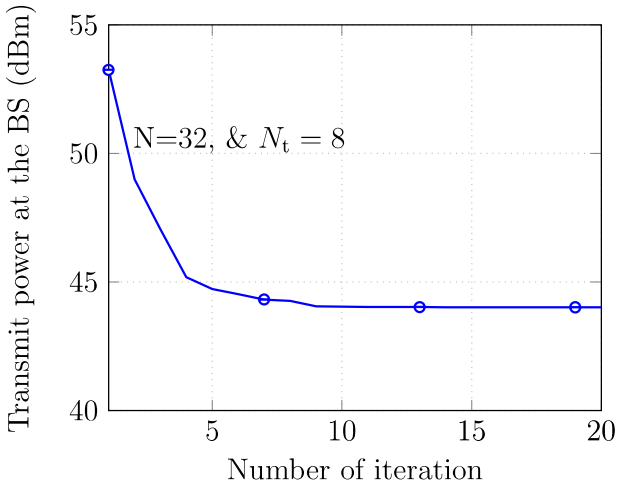

FIGURE 5.3: BS's tranmit power versus number of iteration.

In the proposed alternating optimization algorithm, both problem (P4) and problem (P5) are alternatively solved until the convergence metric is triggered. The value of SNR in problem (P4) is based on a solution $\mathbf{w}, \mathbf{\Phi}$ as $f(\mathbf{w}, \mathbf{\Phi})$. If there exists a solution to problem (P4) then $\mathbf{w}^{(t)}, \mathbf{\Phi}^{(t)}$ and $\mathbf{w}^{(t+1)}, \mathbf{\Phi}^{(t+1)}$ are both feasible solutions to the problem (P4) in the t-th and $(t+1)$th iteration, respectively.

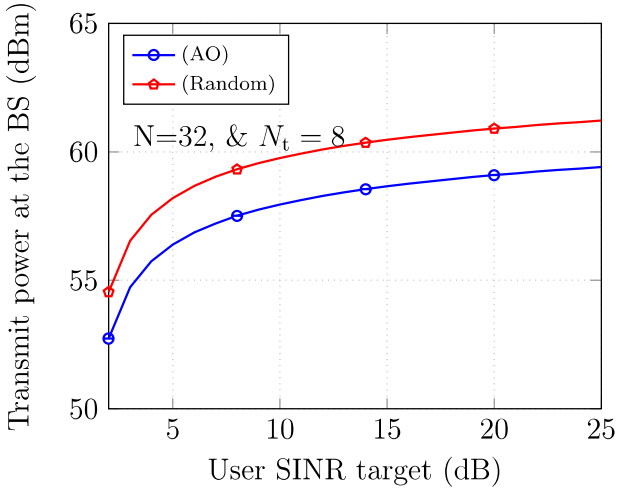

FIGURE 5.4: BS's tranmit power versus SINR target for two users.

5.3.4 Complexity of algorithms

The computational complexity of solving problem (P4) is $\mathcal{O}(KN_{\mathrm{t}}^{3.5})$ and the computational complexity of solving the problem 5.42 is $\mathcal{O}((N+1)^{3.5})$. Therefore, the proposed algorithm to achieve convergence, computational complexity is $\mathcal{O}(z(N_{\mathrm{t}}^{3.5}+(N+1)^{3.5}))$, where z is the number of iterations to achieve convergence.

5.4 Simulation Results and Discussions

In this section, the simulation results of the proposed system with three users are presented. The NU and FUs' distances from the BS to users are $d_{\mathrm{B}\mathcal{U}_1} = 40$m, $d_{\mathrm{B}\mathcal{U}_2} = 100$m and $d_{\mathrm{B}\mathcal{U}_3} = 120$m and its power coefficients are $\alpha_1 = 0.2$, $\alpha_2 = \alpha_3 = 0.8$ and $\kappa_1 = 0.1$, $\kappa_2 = 0.4$,$\kappa_3 = 0.5$. Further, the distance between the BS and RIS is $d_{\mathrm{BR}} = 10$m and distance between RIS to users are $d_{\mathrm{R}\mathcal{U}_1} = 30$m, $d_{\mathrm{R}\mathcal{U}_2} = 90$m and $d_{\mathrm{R}\mathcal{U}_3} = 110$m. The BW of system is set as 1 Hz, $\eta = 3.5$, $\beta = 3$, Rician factor K = K$_i$ = 1 and noise power spectral density is -150 dBm/Hz. The reference channel power gain is -30 dB at distance of 1m [93].

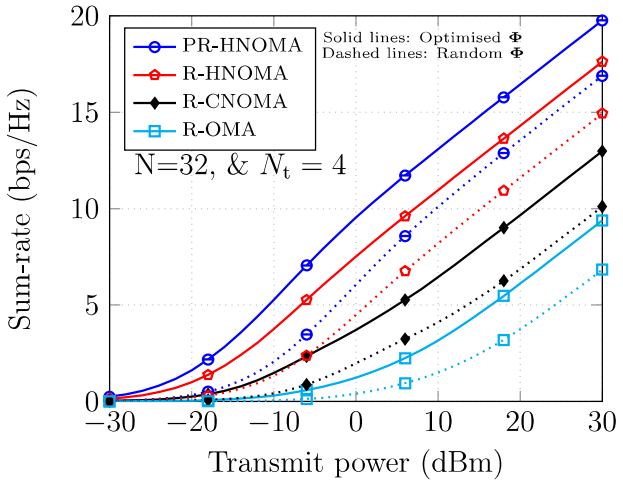

FIGURE 5.5: Sum-rate performance of three different schemes PR-HNOMA,R-HNOMA and R-NOMA with R-OMA systems.

Figure 5.5 shows the sum-rate comparison of the PR-HNOMA with three different R-HNOMA, R-CNOMA, and R-OMA schemes. Each scheme varied with the transmit power P_{t}, between -30dBm to 30dBm with $N_{\mathrm{t}} = 4$ and $N = 32$. The proposed PR-HNOMA shows better sum-rate performance over the other schemes, as observed in Figure 5.5. Since the PR-HNOMA is free from interference, it has a low receiver complexity. It is also observed that the optimized phase using SDR and AO yields an improved performance over random phase settings ($\phi \in [0, 2\pi]$). Moreover, each scheme's sum-rate improves as P_{t} increases.

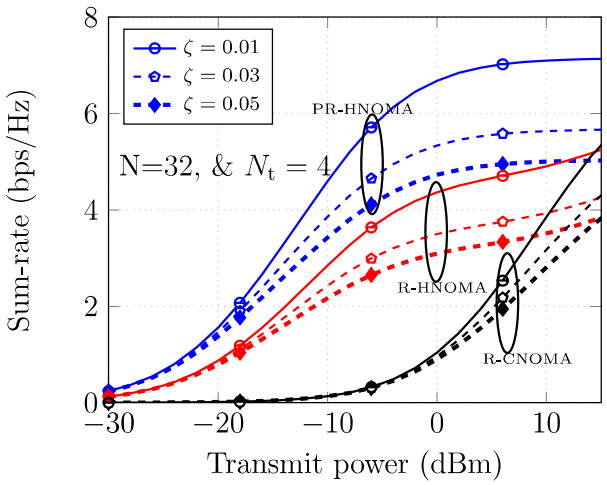

FIGURE 5.6: Sum-rate performance of three different schemes of NOMA under the imperfect SIC.

Figure5.6 illustrates the impact of imperfect SIC. It is observed from Figure5.6, the imperfect SIC degrades the sum-rate in all considered schemes due to FUs' interference. Further, the proposed PR-HNOMA has higher sum-rate than the R-HNOMA and R-CNOMA, as observed in Figure5.6. Since $\mathcal{U}_2$ and $\mathcal{U}_3$ are affected by strong user interference in R-HNOMA and R-CNOMA, respectively, all three users are suffered with strong user interference. In Figure 5.7 the sum-rate performance of the PR-HNOMA is compared using the following different beamforming techniques: (1) joint BS and RIS beamforming using (SDR) and (AO); (2) BS-User MRT beamforming as $\mathbf{w}_k = \sqrt{\mathrm{P}_t}\frac{\mathbf{h}_k}{\|\mathbf{h}_k\|}$ by considering only direct channel from the BS to users

(BS-User MRT); (3) BS-RIS MRT beamforming as $\mathbf{w} = \sqrt{\mathrm{P}_t}\frac{\mathbf{H}}{\|\mathbf{H}\|}$ by considering BS-RIS rank one channel (BS-RIS MRT); (4) Random phase shifting as $\phi \in [0, 2\pi]$; and (5) Without RIS as $\mathbf{w}_k = \sqrt{\mathrm{P}_t}\frac{\mathbf{h}_k}{\|\mathbf{h}_k\|}$ (Without RIS). From Figure5.7, it is observe that the proposed SDR and AO techniques are outperformed in the PR-HNOMA, and also observed that the BS-RIS MRT scheme achieves a better sum-rate than the BS-user MRT, as the reflected signal from the RIS is much stronger than the direct signals between BS and users.

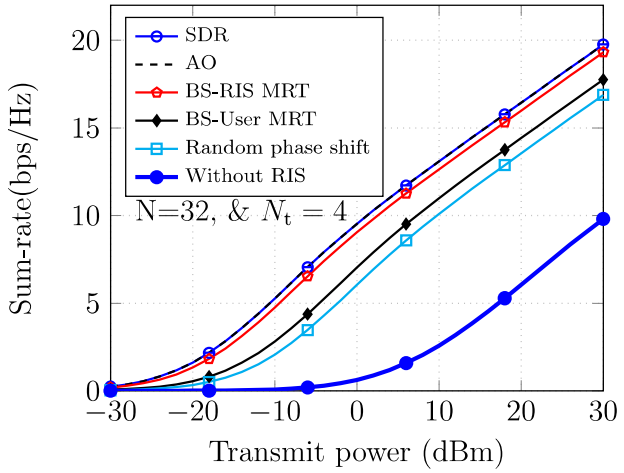

FIGURE 5.7: Impact of different transmit beamforming on the sum-rate in the PR-HNOMA.

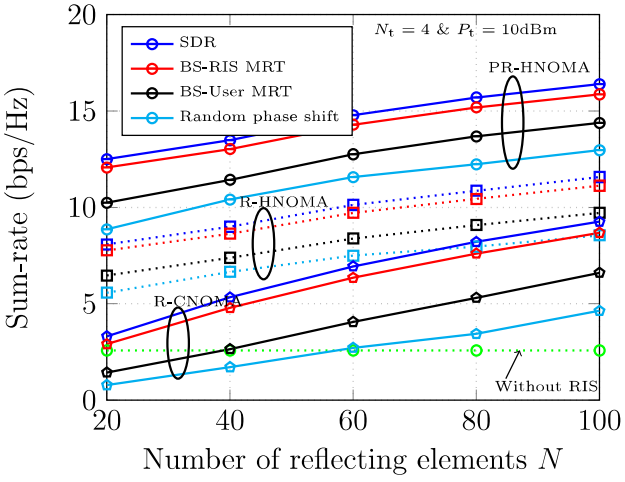

FIGURE 5.8: Sum-rate performance with number of reflecting elements at the RIS.

Further, Figure 5.8 shows the sum-rate performnace versus the number of reflecting elements, N performance for PR-HNOMA, R-HNOMA, and R-CNOMA with different transmit beamforming techniques. The sum-rate of each scheme is enhanced, as the number of reflecting elements increases, since RIS creates a virtual MIMO channel between the BS and RIS, and increasing the number of reflecting elements, N enhances the array gain and reflecting beamforming gain are enhanced. Therefore, the PR-HNOMA experiences N^2 beamforming gain. However, in a conventional MRT scheme, beamforming gain depends on only active transmit antennas. The results of the summary suggest that the performance of the proposed RIS-assisted user-pairing HNOMA system is improved by the implementation of active and passive beamforming. This is achieved through the use of SDR and AO algorithms.

5.5 Summary

In this chapter a energy and spectrally efficient RIS-assisted user-paring HNOMA (PR-HNOMA) system has been proposed by considering more FUs than NUs in a cluster. The joint optimization of transmit beamforming at BS and passive beamforming at RIS was considered by using SDR and AO techniques. Simulation results showed that the proposed PR-HNOMA system's sum-rate performance is better than to the conventional R-HNOMA, R-CNOMA, and R-OMA systems under the imperfect SIC. Further, the sum-rate performance in BS-RIS MRT beamforming is better than other beamforming techniques such as BS-User-MRT. Finally, the sum rates of PR-NOMA, R-NOMA, R-CNOMA, and R-OMA schemes has grown linearly as the number of reflecting elements increases.